# Effect of Hygrothermal Aging on Interfacial Reliability of Silicon/Underfill/FR-4 Assembly

Xunqing Q. Shi, Yanlie L. Zhang, Wei Zhou, and Xuejun J. Fan

***Abstract*—The reliability issues have been converted to the underfill adjacent interfaces since the introduction of the underfill to flip chip package in 1990's. Both thermal cycling and hygrothermal conditioning severely attack the interfaces to delaminate. The moisture migrating into the underfill decreases the adhesion strength, swells to deform the assembly, and weakens the mechanical and thermal properties of the material. In this study, interfacial reliability of a silicon/underfill/FR-4 assembly exposed at 85 °C/85%RH was studied using moiré interferometry and micro-digital image speckle correlation ($\mu$-DiSC) techniques. A thermal aging study was simultaneously performed to understand the long-term reliability of the assembly. The results showed that the thermal aging relieved the stresses induced by hygrothermal swelling mismatch between dissimilar materials involved, whereas increased the strains induced by hygrothermal swelling. It indicated the time effect is not negligible when the assembly is subjected to the moisture conditioning, otherwise, the deformation induced by the swelling could be overestimated. The $\mu$-DiSC technique was applied to measure the critical interfacial fracture toughness of the silicon/underfill interface. The results showed that the moisture could significantly reduce the interfacial strength due to the break of hydrogen bonding. By combining the moiré and $\mu$-DiSC results, it was concluded that the hygrothermal loading could increase the possibility of interfacial delamination in a flip chip package. Finally, the morphologies of the fractured surface were studied with the aid of scanning electron microscope. Remarkable changes of the failure mode were observed.**

***Index Terms*—Coefficient of thermal expansion (CTE), flip chip on board (FCOB), input/output (I/O).**

## I. Introduction

FLIP chip on board (FCOB) has been widely used because of its merits, such as high input/output (I/O), and small package size. The package is plastically underfilled by epoxy-based material to minimize the coefficient of thermal expansion (CTE) mismatch between the chip and substrate as well as to protect the solder connections from the environmental attack. The reliability issues have been converted to the underfill adjacent interfaces [1]. Although many efforts have been done to address the reliability issues of the package, it was found that the package remained susceptible under the environmental attack, such as moisture conditioning especially under the elevated temperature.

Moisture migrating into the plastic packages induces hazardous effects on the package reliability. In general, the moisture induced swelling, degradation of material properties, the popcorn and the loss of interfacial strength aggravate the possibility of interfacial delamination during the manufacturing processes and operation conditions. Polymeric materials swell at different rates upon absorbing moisture while the inorganic material does not swell. The different swelling rates induce the strain and stress, same as CTE mismatch [2]. Secondly, moisture alters the thermal as well as mechanical properties of the organic materials, such as CTE, $T_g$ and Young's modulus. This alteration induces severe thermal stresses inside the plastic packages. Thirdly, the vapor pressure is known to be responsible for the eventual popcorn cracking of the plastic integrated circuit (IC) packages. The stress generated by the vapor pressure during the solder reflow can severely initialize the inherent defects, such as void and weak joint, to delaminate at the interface [3]. The vapor pressure evolution and model study have been well established based on a micromechanics approach [3]. Last but not least, moisture has an adverse effect on the interfacial adhesion, which can accelerate the delamination by deteriorating the polymer interfaces within the package [4]–[6]. A comprehensive review of moisture induced failures in electronic packaging was presented in [2].

With the aid of finite element analysis software, many studies have been conducted to understand the hygrothermal behavior of plastic packages. The results are irradiative to the knowledge of moisture induced reliability problems. With an appropriate thermal-moisture analogy, moisture diffusion in the polymeric material can be modeled based on thermal diffusion function of the finite element software, whose approach gave good prediction of acceleration factors compared to the experimental values [7], [8]. To solve the discontinuity of moisture concentration between different adjacent materials, recently a more general method so-called "direct concentration approach (DCA)" has been developed to investigate the moisture absorption, desorption and diffusion during soldering reflow for a stack-die chip scale package [7].

On the other hand, it was reported that the decrease of interfacial adhesion was up to 50% after long period of aging [4]. It is of interest that a limit exists on moisture induced strength degradation beyond which no further degradation happens [9]. The possible answer is that the degradation is related to the nature of moisture diffusion, which is Fickian.

Manuscript received February 26, 2005; revised October 30, 2007. This work was supported by the National Natural Science Foundation of China under Grants 10572010 and KM200610005013. This work was recommended for publication by Associate Editor K. Zhang upon evaluation of the reviewers comments.

X. Q. Shi is with the College of Mechanical Engineering and Applied Electronics Technology, Beijing University of Technology, Beijing 100022, China (e-mail: xqshi@ieee.org).

Y. L. Zhang and W. Zhou are with the Precision Engineering and Nanotechnology Center, School of MPE, Nanyang Technological University, Singapore 639798 (e-mail: wzhou@cantab.net).

X. J. Fan is with the Department of Mechanical Engineering, Lamar University, Beaumont, TX 77710 USA (e-mail: xuejun.fan@lamar.edu).

Color versions of one or more of the figures in this paper are available online at http://ieeexplore.ieee.org.

Digital Object Identifier 10.1109/TCAPT.2008.916801

These efforts have remarkably improved the knowledge of moisture induced interfacial problem. However, in order to improve the interfacial reliability, apart from the numerical analysis, it is necessary to realistically understand the failure mechanism of the FCOB package under the hygrothermal aging by using accurate experimental measurement technique. Moreover, in the author's best knowledge, few studies have taken the time effect into consideration even though the underfill exhibits the viscoelasticity under hygrothermal aging, which is normally carried out under the high temperature for long time. The difficulties of experimental work may exist inherently since the hygrothermal deformation is a three-dimensional problem with the consideration of the nature of moisture diffusion. However, it is estimated that, if the structure response under the saturated condition with $C_{\mathrm{sat}}$ can be understood, it is possible to evaluate the reliability status of the assembly under the varying unsaturated moisture concentration. Therefore, initial study is required to be carried out based on two-dimensional *in-situ* measurement with the assumption of saturated moisture concentration on the in-plane surface, consistent with boundary condition applied in the finite element analysis. Further, the delaminated assembly has to be especially concerned since the generation of delamination or the existence of inherent defects is supposed to further degrade the thermal, mechanical and electrical integrity of the package. However, fracture behaviors under the moisture conditioning have not been well elaborated so far. The experimental technique assorting with appropriate fracture mechanics theory is thought to be a bottleneck in the study of fractured package.

In this study, a developed moiré interferometry system with interfacial fracture mechanics method was used to investigate the fracture behavior of a silicon/underfill/FR-4 assembly under the hygrothermal aging. In order to study the time effect on the delaminated assembly, the thermal aging study was simultaneously implemented. The representative deformation and stress intensity factors (SIF) showed that the moisture induced swelling played a crucial role on structure interfacial reliability apart from the CTE mismatch between the materials. It is more of importance that the isolation of the time effect and the hygroscopic swelling effect indicated that the time effect was beneficial to alleviate the fracture potentiality. The positive aspect of the time effect implied that the conventional finite element analysis might overestimate the moisture-induced stress and threat if the time effect was not included. Further, efforts were made to measure the critical interfacial fracture toughness between silicon/underfill using the micro-digital image speckle correlation ($\mu$-DiSC) technique and to evaluate the possibility of fracture after the hygrothermal loading. The results showed the moisture content diffusing into the assembly had greater potentiality on interfacial delamination compared to dry specimens. Finally, the fracture morphologies were studied using a scanning electron microscope (SEM), remarkable changes of the failure mode were observed.

## II. Interfacial Fracture Mechanics Approach

Interfacial fracture mechanics approach is usually employed to determine the resistance of an interface to fracture [10]. For the interface crack shown in the Fig. 1, the relative crack displacement at a distance of $r$ behind the crack-tip ($\theta = \pi$) [11]

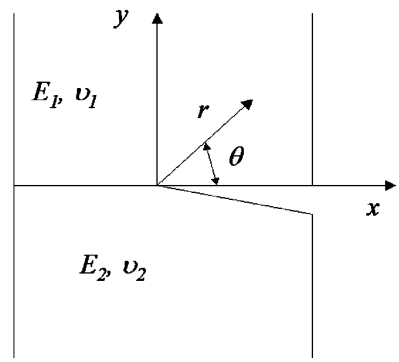


Fig. 1. Interface crack problem.

$$\delta = \delta_y + i\delta_x = \frac{8}{(1+2i\varepsilon)\cosh(\pi\varepsilon)}\sqrt{\frac{r}{2\pi}}\frac{K'}{E^*}\left(\frac{r}{L}\right)^{i\varepsilon} \quad (1)$$

where $\delta_x$ and $\delta_y$ are the crack-tip opening displacements (CTODs) in the $X$ and $Y$ direction, respectively; $\varepsilon$ is related to material properties defined in [12]. $E^*$ is the effective Young's modulus given by

$$\frac{2}{E^*} = \frac{1}{\overline{E_1}} + \frac{1}{\overline{E_2}} \quad (2)$$

with $\overline{E_i} = E_i/(1-\nu_i)$ for the plane strain and $\overline{E_i} = E_i$ for the plane stress. $K'$ is the nominal complex interfacial stress intensity factor (SIF) defined as

$$K' = K'_1 + iK'_2 \quad (3)$$

where $K'_1$ and $K'_2$ are the nominal mode I and mode II SIF, respectively.

By solving (1), the individual SIF is obtained

$$\begin{cases} K'_1 = \frac{\{A\cos[\varepsilon In(\frac{r}{L})]+B\sin[\varepsilon In(\frac{r}{L})]\}}{D} \\ K'_2 = \frac{\{B\cos[\varepsilon In(\frac{r}{L})]-A\sin[\varepsilon In(\frac{r}{L})]\}}{D} \end{cases} \quad (4)$$

where

$$\begin{cases} A = \delta_y - 2\varepsilon\delta_x \\ B = \delta_x + 2\varepsilon\delta_y \\ D = \frac{8}{E^*\cosh(\pi\varepsilon)}\sqrt{\frac{r}{2\pi}} \end{cases}. \quad (5)$$

It is of importance that once the deformations around the crack-tip are known, it is possible to deduce the $K'_1$ and $K'_2$. Noted that the $K'_1$ and $K'_2$ derived in (4) are nominal SIFs with respect to a distance $r$ away from the crack-tip. The exact solutions of $K_1$ and $K_2$ at the crack-tip are supposed to be acquired through extrapolation according to nominal SIFs as a function of distance $r$ away from the crack-tip [13]. The effective stress intensity factor $K_{eff}$, is related to the mode I and mode II stress intensity factors by [14]

$$K_{eff} = \sqrt{K_1^2 + K_2^2} \quad (6)$$

and the phase angle is defined as

$$\psi = \tan^{-1}\left(\frac{\mathrm{Im}(Kl^{i\varepsilon})}{\mathrm{Re}(Kl^{i\varepsilon})}\right)_{\beta\neq 0}. \quad (7)$$

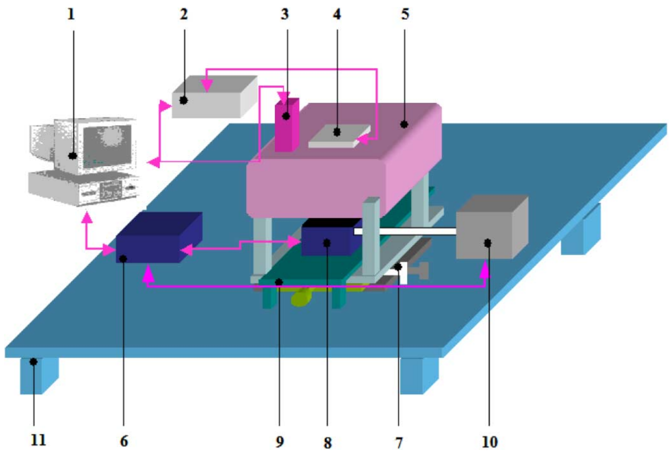


Fig. 2. Schematic diagram of the $M^3I$ system: 1: computer; 2: driver of phase shifter; 3: microscopic imaging device; 4: phase shifter; 5: moiré interferometer; 6: temperature and humidity controller; 7: six-axis fixture; 8: miniature humidity chamber; 9: chamber support; 10: ultrasonic humidity excitation; 11: optical table.

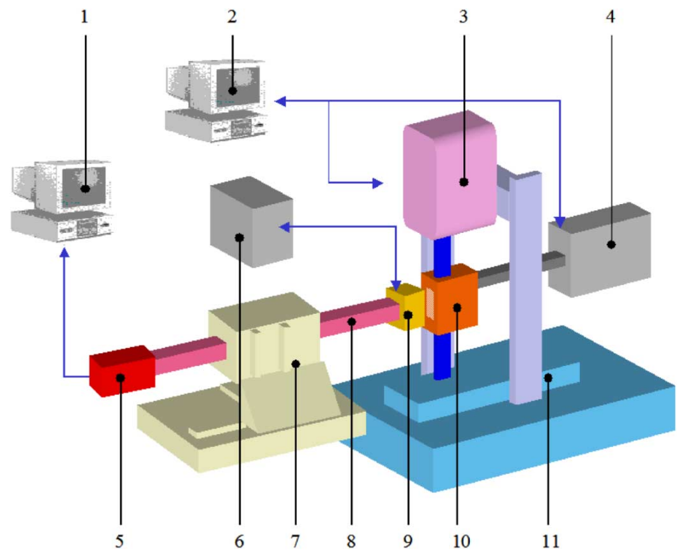


Fig. 3. Schematic diagram of the integrated $\mu$-DiSC system: 1: computer 1; 2: computer 2; 3: INSTRON micro tester; 4: Heater; 5: CCD camera; 6: light source; 7: six-axis fixture; 8: microscope; 9: illuminator; 10: attemperator; 11. pedestal.

Although the underfill used in this study exhibited significant viscoelastic behavior, the previous investigation demonstrated the validity of linear interfacial fracture mechanics for the interfacial strength analysis [15].

## III. Photomechanics Measurement Techniques

### A. Moiré Interferometry

In this study, an integrated multifunctional micro-moiré interferometry $(M^3I)$ system was developed, by combining moiré interferometry (MI) technique with thermoelectric heating and cooling technique (for thermal cycling), humidity system (for hygrothermal aging), and microscopic imaging technique, to investigate the interfacial reliability of a silicon/underfill/FR-4 assembly. The schematic diagram of $M^3I$ system is shown in Fig. 2. A miniaturized moisture chamber with ultrasonic humidity excitation was developed to control the hygrothermal conditions within the error of 0.1 °C and 1%RH.

With the system, U and V field moiré fringe patterns can be obtained and the displacements and strains can be determined by [16]

$$U(x,y) = \frac{N_x(x,y)}{2f} \tag{8a}$$

$$V(x,y) = \frac{N_y(x,y)}{2f} \tag{8b}$$

$$\varepsilon_x(x,y) = \frac{\partial U(x,y)}{\partial x} = \frac{1}{f}\left[\frac{\partial N_x(x,y)}{\partial x}\right] \tag{9a}$$

$$\varepsilon_y(x,y) = \frac{\partial V(x,y)}{\partial y} = \frac{1}{f}\left[\frac{\partial N_y(x,y)}{\partial y}\right] \tag{9b}$$

$$\begin{aligned}\gamma_{xy}(x,y) &= \frac{\partial U(x,y)}{\partial y} + \frac{\partial V(x,y)}{\partial x} \\ &= \frac{1}{f}\left[\frac{\partial N_x(x,y)}{\partial y} + \frac{\partial N_y(x,y)}{\partial x}\right]\end{aligned} \tag{9c}$$

where $f$ is the frequency of specimen grating; $N_x(x,y)$ and $N_y(x,y)$ are the fringe orders in the $U(x,y)$ and $V(x,y)$ field moiré patterns, respectively; $\epsilon_x(x,y)$, $\epsilon_y(x,y)$ and $\gamma_{xy}(x,y)$ are the normal strain fields in $x$ and $y$ directions and the shear strain field in the $x$–$y$ plane, respectively.

### B. Digital Image Correlation (DIC)

Micro-digital image speckle correlation ($\mu$-DiSC) is a technique to measure displacement by correlating with a pair of digital speckle patterns obtained at two different loading conditions and searching for the maximum correlation coefficient $C$[17]. Since the common coarse-fine search algorithm uses the full-field search and tries many combinations of deformation variables, the calculation becomes time-consuming. Following our previous work [18], [19], a developed line search algorithm were used to improve search accuracy and computational time, which made real-time measurement possible. Further, the bicubic spline interpolation method was employed to smoothen the surface of gray level distribution and determine the maximum correlation coefficient C. The overall arrangement of the experiment setup is schematically shown in Fig. 3.

## IV. Experimental Details

### A. Specimen Preparation

In this study, silicon/underfill/FR-4 assemblies were prepared as shown in Fig. 4. The solder joints were removed in order to simplify the study, since it was reported that solder joints played a small role in the warpage of underfilled flip chip package while the underfill epoxy played a dominant role [20]. The attention was drawn on the interfacial delamination behavior between silicon/underfill. The assembly consisted of three materials, namely, silicon, underfill and FR-4. A commercialized epoxy based underfill material supplied by Loctite was used in this study. The composition of the material was 60% epoxy with 40% silica filling sizing from 1 to 4 $\mu$m. The glass transition temperature $(T_g)$ of the underfill was determined to be 105 °C using differential scanning calorimeter (DSC) [21]. The material properties for underfill, silicon and FR-4 are listed in previous paper [22]. For the underfill material, the linear relation

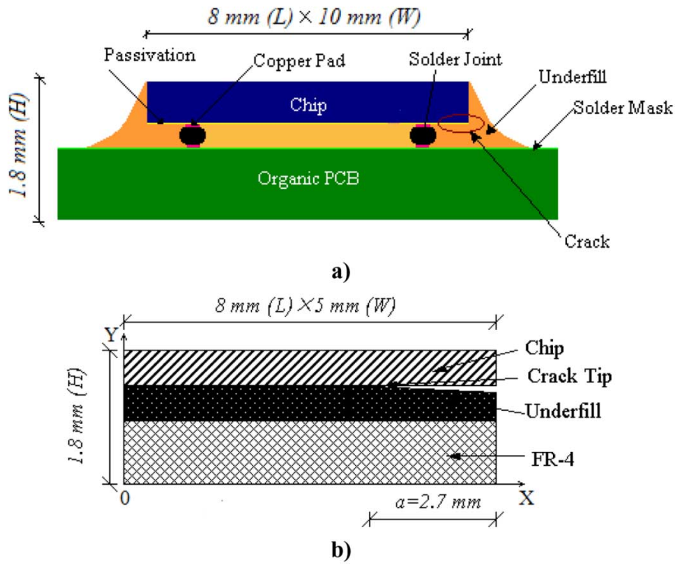


Fig. 4. Schematic diagram of the assembly to be studied: (a) flip chip package and (b) silicon/underfill/FR-4 assembly.

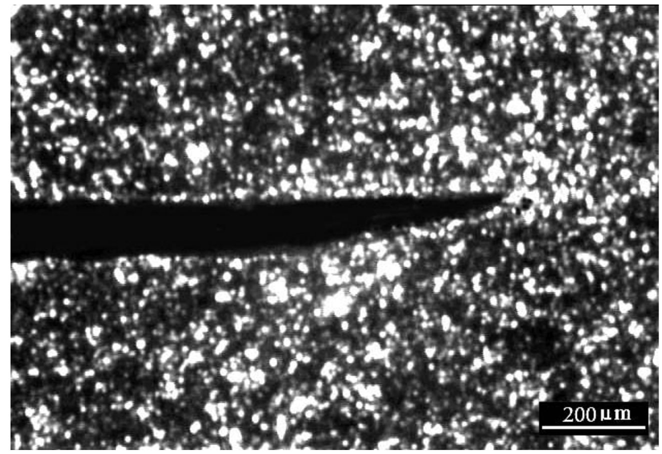


Fig. 5. Typical digital speckle pattern of SBN at the crack tip.

exists between hygroscopic stain and moisture concentration. Therefore, the coefficient of moisture expansion (CME) of the underfill is determined to be 0.31cc/g using thermal gravimetric analyzer (TGA) and thermomechanical analyzer (TMA).

The dimensions of the assembly were 8 mm(L)×5 mm(W)× 1.8 mm(H). The thickness of the underfill was 0.5 mm. It was demonstrated not to result in enhanced resistance to progressive debonding under temperature loading [23]. A pre-crack was prepared at the silicon/underfill interface by using a piece of silicon rubber film with thickness of 20 $\mu$m. The length $a$ and the ligament of $w$ ahead of the crack tip were respectively 2.7 and 5.3 mm, satisfying $a, w > H + h + t$, where $H$, $h$, and $t$ are the thickness of FR-4, silicon wafer and underfill respectively. The selection of these dimensions was to neglect edge effects on loading. Under these situations, a steady state solution was valid and the dependence of stress intensity factors (SIFs) on the crack length can be eliminated [24].

A dispenser and a curing oven were employed to prepare the assembly. By following flip-chip packaging process, an optimized curing condition was defined to be 165 °C for 8 min. Due to the capillary effect, underfill was dispensed into the gap between the silicon and FR-4. When the specimen was partially cured, the rubber was quickly removed from the specimen and a sharp crack was fabricated. After fabrication, each assembly was carefully polished with a fine SiC paper to remove excessive underfill and to obtain the desired dimensions.

### *B. Measurement of Thermal and Hygrothermal Deformation*

The $M^3I$ system was employed to determine the deformation field around the interfacial crack-tip of the assembly subject to thermal and hygrothermal loadings. Specimen grating with a frequency of 1200 lines/mm was replicated onto the surface of the assembly at room temperature. The assembly was then put into the miniaturized moisture chamber with the hygrothermal loading conditioned at 85 °C/85%RH for 168 h. The moiré fringe patterns were captured at the times of 0, 1, 3, 7, 11, 24, 48, 96, and 168 h.

In order to eliminate the time effect, i.e., creep of underfill material, a thermal aging test was carried out on the same assembly and the moiré fringe patterns were acquired at the time intervals. The aging temperature was 85 °C. The humidity level under the thermal aging test was 18%, which was expected to cause negligible moisture absorption in the assembly.

### *C. Determination of Critical Interfacial Fracture Toughness*

The DIC technique was combined with a sandwiched brazil-nit (SBN) fixture for characterization of the critical interfacial fracture toughness of silicon/underfill interface under different mixed-mode loading conditions. The sandwich structure was made of silicon/underfill/silicon with a 4 mm pre-crack manufactured at the silicon/underfill interface. The thickness of the underfill was chosen to be 0.5 mm, which is consistent with the thickness in the moiré experiment. The SBNs were aged under 85 °C/85%RH in a hygrothermal chamber for 168 h beforehand. Artificial speckle patterns were subsequently generated on the specimen surface using white paint and carbon particles to create images with high contrast of gray level, as shown in Fig. 5.

The interfacial fracture tests on the samples were conducted with INSTRON micro-tensile machine at room temperature. A high resolution CCD camera was used to capture speckle patterns at different load levels. With the curve, the speckle pattern at the load level where the interface crack opened could be obtained. This pattern and the initial speckle pattern were used as undeformed and deformed images. With the correlation software, the displacement fields around the crack-tip could be determined [18].

## V. Results and Discussion

### *A. Hygrothermal Displacement*

The fringe patterns in both $x$ and $y$-direction at the initial state ($t = 0$, 85 °C/dry) and different time intervals were presented in Fig. 6. It was observed that the number of fringe orders increased at the beginning. It was believed to be the result of the swelling of the underfill material upon moisture absorption. When water immigrated into epoxy-based underfill, it broke the interchain bonds by forming hydrogen bonds with chain interruption [25]. The formation of hydrogen bonds permitted the resin network to

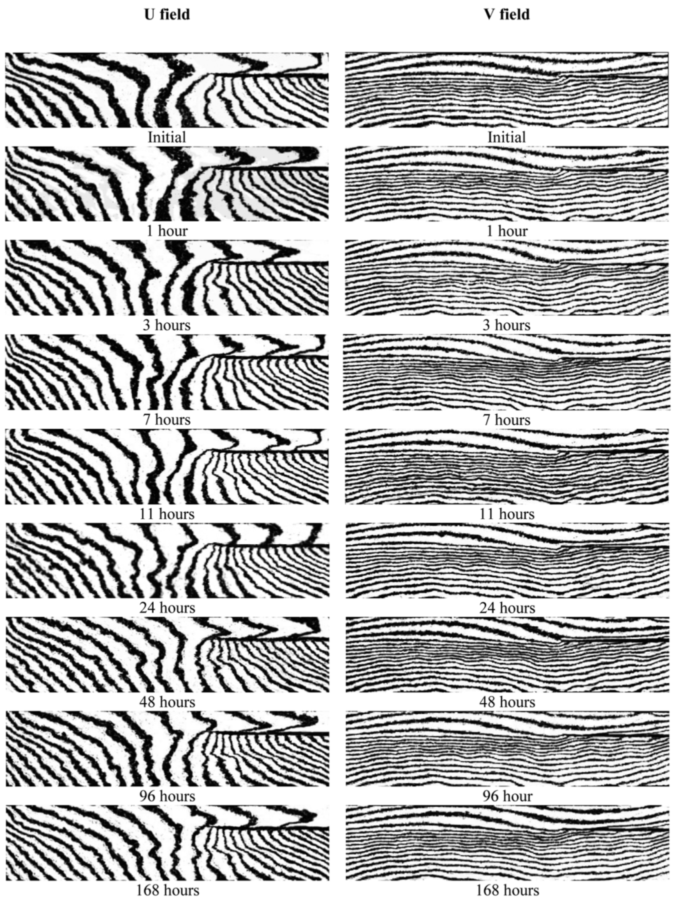


Fig. 6. Fringe patterns during hygrothermal aging under 85 °C/85%RH.

expand through relaxation of the stresses produced by osmotic pressure [26]. Afterwards, the increase of fringe orders was not that significant. First, it was found from the experimental results that the absorption property of the underfill was Fickian as shown in Fig. 7. Second, the modulus of underfill material gradually decreased due to the viscoelasticity of underfill. The combination of both factors lead to inapparent increase of moiré pattern. The characterization procedures of the moisture properties of the underfill have been described in detail in JEDEC standard JEDEC 22-A120. Note that since the moisture diffusion of underfill material in the sandwiched specimen was predominantly one-dimensional, the moisture uptake was described with (10), which was an asymptotic curve as a function of time [27]

$$\frac{M_t}{M_{\text{sat}}} = 1 - \frac{8}{\pi^2} \sum_{n=1}^{\infty} \frac{1}{(2n+1)^2} \exp\left[-\frac{D_z t}{z_0^2}[(2n+1)\pi]^2\right] \quad (10)$$

where $D$ is the diffusion coefficient, $z_0$ is the total film thickness, $M_t$ is total mass of the diffusing substance absorbed by the sample at time $t$, and $M_\infty$ is the equilibrium mass of the absorbed substance.

It was, therefore, thought that the initial majority of moisture uptake caused most of swelling in the underfill. With the slowing of moisture absorption for long period of time, the corresponding swelling induced deformation became inconspicuous. As an evidence, the normal and shear strains at the leftward edge of silicon/underfill interface were determined with

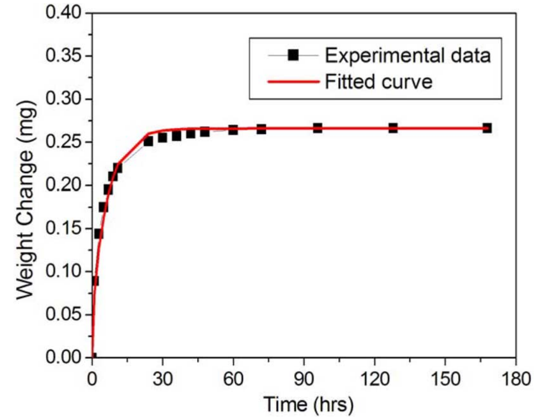


Fig. 7. Weight gain and Fickian curve fit at 85 °C/85%RH for underfill.

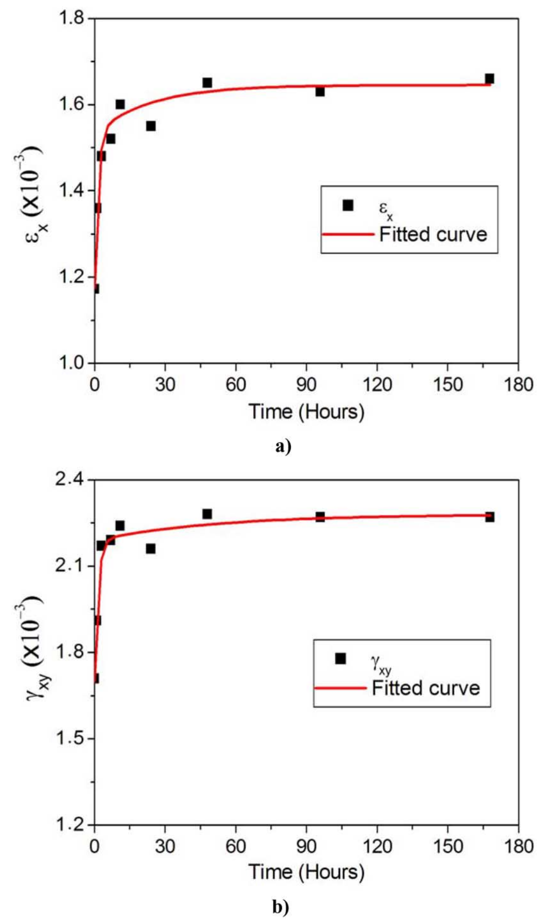


Fig. 8. Strain gradients at the leftward of silicon/underfill interface in hygrothermal aging (85 °C/85%RH) (a) $\varepsilon_x$ and (b) $\gamma_{xy}$.

(9). The results were plotted in Fig. 8. As seen, the strains increased as time increased. Both normal strain and shear strain showed similar trends, which was in asymptotic manner. They were analogous to the moisture diffusion in underfill since moisture absorbed in the underfill has physical reaction with interchain bonds and therefore causes swelling [25]. This observation was also physically, apart from chemical point of view, proved that the swelling of underfill was related to the concentration of moisture diffusion at a certain extent.

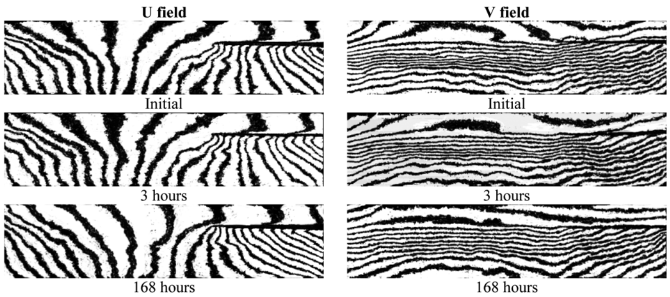


Fig. 9. Representative fringe patterns under the thermal aging test (168 h under 85 °C).

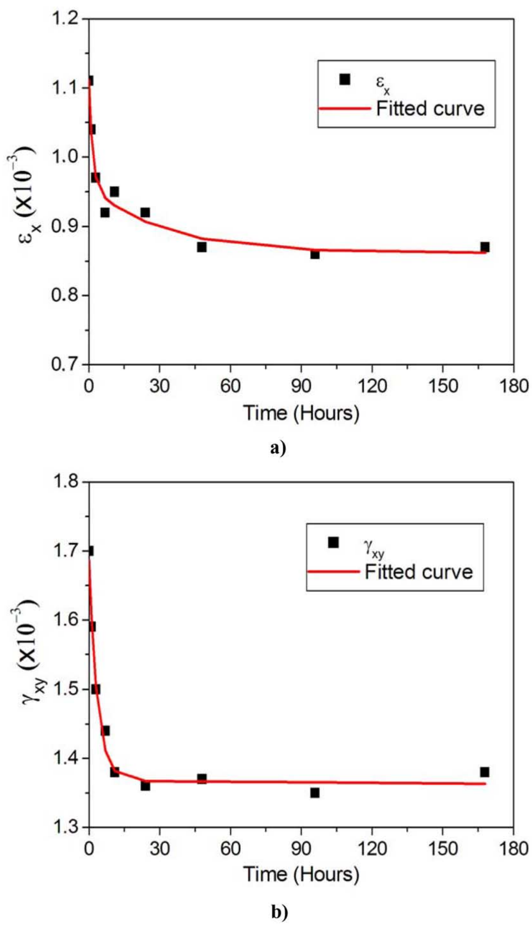


Fig. 10. Strain gradients at the leftward of silicon/underfill interface thermally aged at 85 °C: (a) $\varepsilon_x$ and (b) $\gamma_{xy}$.

## B. Thermal Deformation

The study of thermal deformation was performed to understand the time effect on the reliability of the assembly under the hygrothermal aging. The representative fringe patterns under different intervals were shown in Fig. 9. The normal and shear strains at the leftward of silicon/underfill interface were plotted in Fig. 10. It can be seen from Fig. 9 that, analogous to hygrothermal aging effect, the time effect was significant at the beginning. The strains reduced fast since the stresses caused by thermal mismatch of dissimilar materials were initially large. As the time going on, time effect became not that obvious. Up

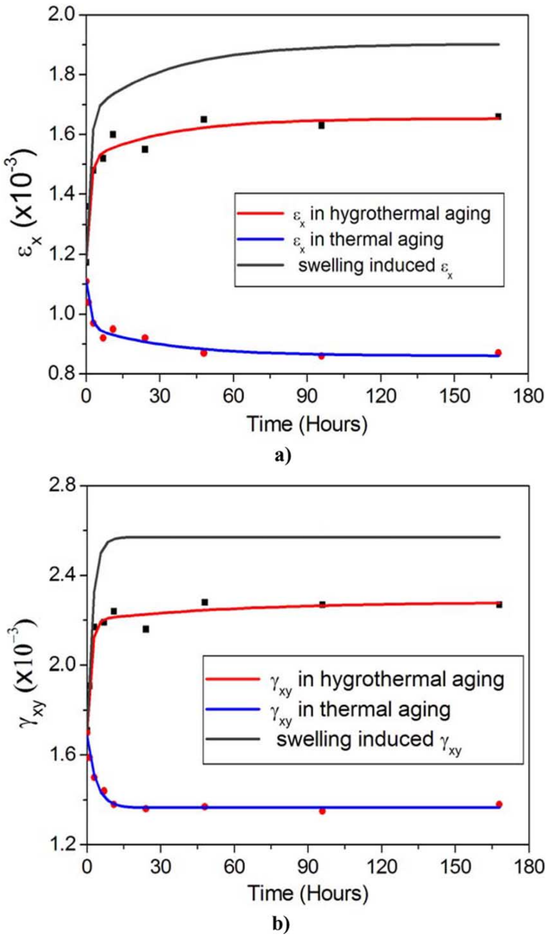


Fig. 11. Swelling induced strains by using superposition method (a) $\varepsilon_x$ and (b) $\gamma_{xy}$.

to 60% to 70% decrease of strains occurred at the beginning 3 h, while the remainder released within a relatively long period due to the stress relaxation. Therefore, it was believed that the thermal aging, which was related to stress relaxation during aging under the high temperature, helped to gradually reduce the magnitude of deformation of sandwiched structure. Wang *et al.* [28] presented similar results observed that a FCOB assembly without pre-crack exhibited significant time effect under high aging temperature, and stress relaxation happened rapidly at the very beginning of several hours.

The superposition principle has been widely used to separate the deformation caused by thermal aging from that caused by the hygroscopic swelling [1]. With the consideration of stress relaxation, the actual swelling induced strains were expected to be greater than those measured in hygrothermal aging, as shown in Fig. 11. In the figure, the losses of strains induced by thermal aging were added to the strains measured in hygrothermal aging. As a result, the values of swelling induce strains were enlarged 20%–30%. It is therefore thought that the time effect should be considered in case of hygrothermal aging, which is beneficial to assembly reliability since it reduces the strains induced by material swelling during moisture immigration. Also it is of necessity to include the time effect when finite element simulation is performed; otherwise the hygrothermal effect might be overestimated in reliability evaluation.

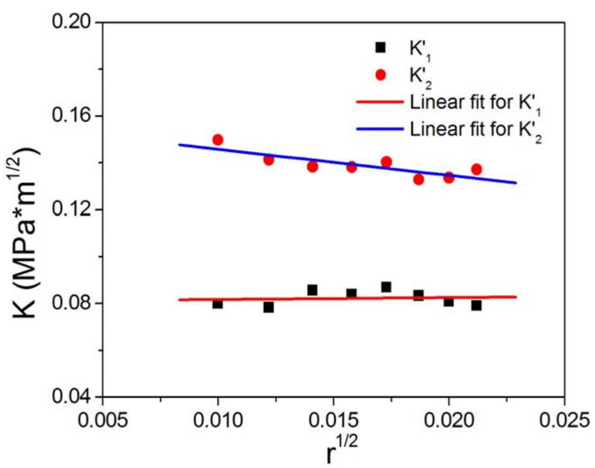


Fig. 12. Representative extrapolation method according to linear relationship under the 85 °C/85% after 168 h.

### C. Fracture Parameters Under Hygrothermal Aging

It is widely reported that the adhesion of interface can markedly reduce after moisture conditioning [29], [30]. In case the interface toughness was measured as a result of hygrothermal aging, it is convenient to quantitatively evaluate the potential of fracture propagation by comparing with the critical interfacial fracture toughness and thus understand the reliability of silicon/underfill interface under the moisture attack.

Based on the displacement fields obtained by the moiré test, the nominal $K_1'$ and $K_2'$ can be determined using (1) to (7) for any given distance $r$ away from the crack-tip. According to (1) to (4), $K_1'$ and $K_2'$ are proportional to $\sqrt{r}$, as shown in Fig. 12. It is noticed that the value of the nominal $K_2'$ increased as the square root of distance $\sqrt{r}$ decreased, while $K_1'$ remained changeless. The $K_1$ and $K_2$ at the crack-tip can be obtained using extrapolation method based on nominal $K_1'$ and $K_2'$ with respect to various distance $r$ away from the crack-tip [13]. As seen in Fig. 12, the nominal SIFs showed an approximate linear relationship with $\sqrt{r}$. The extrapolation method can then be employed to determine the interface toughness at the crack-tip [18]. By curve fitting, the experimental results were extrapolated to $r = 0$, representing the interface toughness $K_1$ and $K_2$ at the crack-tip.

With this method, the values of SIFs at different hygrothermal aging times were determined and the results are presented in Fig. 13. It can be observed that the majority increase of interface toughness occurred at the early stage of aging, which is the same as the strain gradients calculated at the interface. $K_1$ increased 33% and $K_2$ increased 23%, respectively. Both $K_1$ and $K_2$ increased in the asymptotic manner, which were similar to the moisture diffusion nature in the underfill material. On the other hand, the asymptotic curve suggested that the change of the fracture behavior induced by moisture absorption was gradual rather than instant, although the in-plane surface measured was in the boundary condition of saturated moisture concentration.

The values of SIF under the thermal aging were determined and the results are plotted in Fig. 14. It is noted that both of the $K_1$ and $K_2$ reduced faster at the beginning. It was thought that the creep behavior of underfill and solder joints greatly relieved the part of stresses and thereby prevented interfaces from

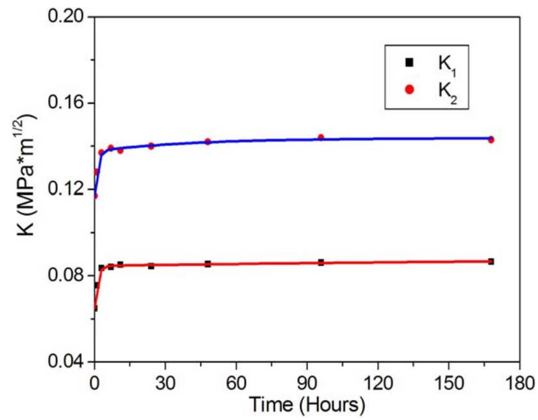


Fig. 13. $K_1$ and $K_2$ with respect to different hygrothermal aging time (85 °C/85%RH).

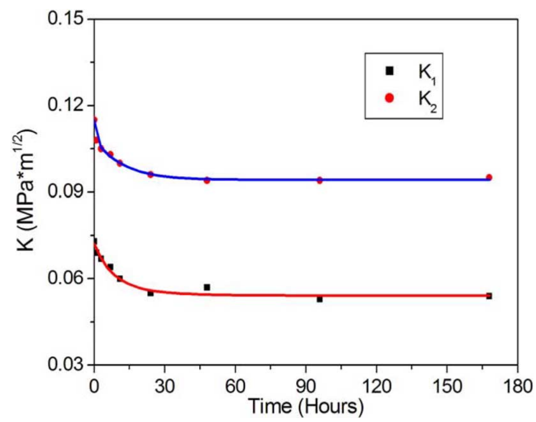


Fig. 14. $K_1$ and $K_2$ with respect to different thermal aging time (85 °C).

cracking [28]. Likely, it was observed in this study, for an assembly with crack, the time effect could play a considerable role on interface toughness although the change of the CTODs were in the small scale.

Therefore, both strains and SIFs showed that the time effect was significant in the hygrothermal aging, especially at the high temperature. In addition, it can be seen that the magnitude of stresses or fracture parameters on time effect was comparable to that on hygrothermal induced swelling. Therefore, the results indicated that the interface toughness induced by the moisture swelling was possible to be overestimated if the time effect was not considered. Since the interface toughness is an important parameter to evaluate the life of assembly during thermal cycling, the greater value of the interface toughness will result in shorter reliability life eventually. Therefore, if the overestimated interface toughness is used to calculate the fatigue life under moisture conditioning, the reliability issues tend to be more severe and give improper estimation. As a result, it is obvious that viscosity (time-temperature behavior) of underfill is of necessity to be included in the reliability study.

### D. Critical Interfacial Fracture Toughness

Since the values of interface toughness under hygrothermal aging were understood, it was easy to quantitatively estimate the possibility of fracture propagation by comparing with the critical interfacial fracture toughness. Based on the $\mu$-DiSC system

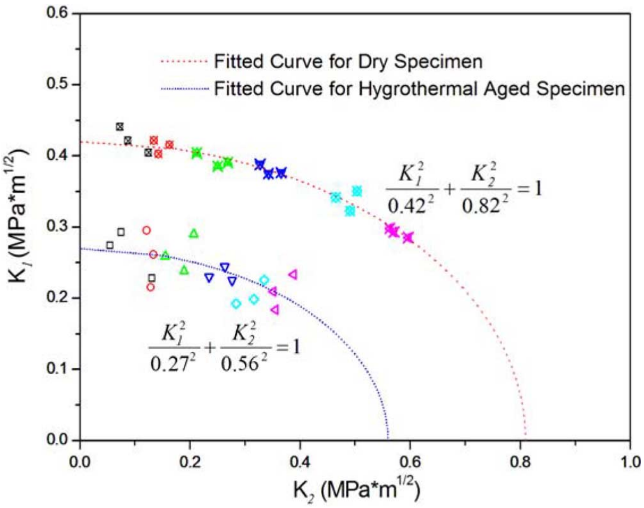


Fig. 15. Critical interfacial fracture toughness of dry and wet (85 °C/85%) SBN specimen.

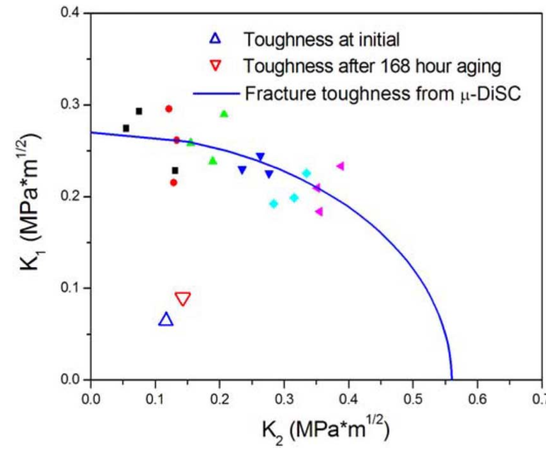


Fig. 16. Failure assessment based on interface toughness and critical interfacial fracture toughness.

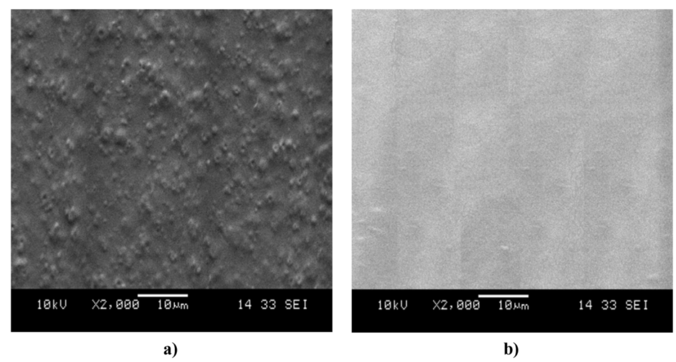


Fig. 17. Fracture morphology of interfacial delamination: (a) interfacial delamination of dry specimen under 125 °C and (b) interfacial delamination of hygrothermal aged specimen under the room temperature.

and interface fracture mechanics, the CTODs obtained in the fracture test were calculated to critical interfacial fracture toughness with respect to different phase angles. Brazil-Nut-specimens were used to achieve this variety. The linear extrapolation method was also examined and subsequently used to obtain SIFs at the crack-tip. The measured results are presented in Fig. 15. It can be seen the critical interfacial fracture toughness $K_{1C}$ and $K_{2C}$ followed the ellipse law with respect to different phase angles. By varying the loading angles, different mode mixities were achieved. However, the $K_{1C}$ decreased slowly when $K_{2C}$ increased by changing the loading angle from 90° to 20°. This indicated that the $K_{1C}$ plays a more critical role in the determination of critical interfacial fracture toughness than $K_{2C}$. After the hygrothermal aging, the critical interfacial fracture toughness decreased significantly compared with the critical interfacial fracture toughness of dry specimen tested at the room temperature [31]. After 168 h of exposure at 85 °C/85%RH, the interfacial adhesion was decreased on average 34.9% for the silicon/underfill interface. Other authors also observed the significant decrease [4], which indicated that the moisture could invade into the defects and remarkably decrease the interfacial strength by intercepting the inter- and intra-molecular hydrogen bonding provided by the hydroxyl groups [25]. Therefore, it demonstrated that the hygrothermal loading would increase the possibility of interfacial delamination in a flip chip package. More decrease happened in mode I (36% for pure mode I fracture and 32% for pure mode II fracture), which means that more severe reliability issues lie in the opening mode. The possible explanation of this phenomenon is due to a displacement type reaction where water molecules displace the polymer chain in the Van-der Waals bonding of the polymer adhesive to the glass surface [32]. In order to demonstrate it, the fracture morphology was to be studied in Section V-E.

Based on the interface toughness $K_1$ and $K_2$ measured by the moiré experiment and critical interfacial fracture toughness $K_{1C}$ and $K_{2C}$ measured by the $\mu$-DiSC system, it is easy to assess the failure possibility by combining the results together. As seen in Fig. 16, the interface toughness fell inside the area defined by the boundary of the critical interfacial fracture toughness and $x$ and $y$ axes, indicating the interface was safe under the 168 h exposure in 85 °C/85%RH hygrothermal environment. However, the figure, on the other hand, indicated that the possibility of the interface delamination increased accompanied with the interface toughness increased around 24.9% after 168 h aging and critical interfacial fracture toughness decreased 34.5%.

### E. Reliability of Silicon/Underfill Interface

It was found that the fracture modes were generally interfacial delamination with respect to all loading angles, which were similar to those of dry specimen tested at 125 °C [31]. However, in the microscopic view, the morphologies of interfacial delamination were surprisingly different. For the delamination happened at 125 °C, it was observed that granular bulges distributed over the whole fractured interface of the underfill part of the dry sample, as shown in Fig. 17(a). It indicated that the chemical bonding was destroyed by high stresses-at-break, which exceeded the local yield stress of underfill material. However, for hygrothermal-aged sample, its fracture morphology showed smooth surface without granulae, as shown in Fig. 17(b). It indicated that the stresses causing debonding were not large enough to make the underfill material yield locally. It is evidence from mechanical point of view that the moisture leads to bonding interception. This observation also demonstrated that moisture could hydrolyze the chemical bonding between underfill and silicon apart from making epoxy-based underfill swell as reported in the moiré experiment.

## VI. Conclusion

In this study, the developed multifunctional micro-moiré interferometry ($M^3I$) system was used to investigate the deformation as well as the interface toughness of a cracked silicon/underfill/FR-4 assembly during 168 h of exposure at 85 °C/85%RH. The thermal aging test at 85 °C was carried out to separate two time-effect, i.e., moisture diffusion induced swelling and stress relaxation caused by the viscoelasticity of underfill. The critical interfacial fracture toughness after hygrothermal aging was characterized using the micro-digital image speckle correlation ($\mu$-DiSC) technique. The corresponding fracture mechanism was studied by scanning electron microscope (SEM).

In strain calculation at the interface of silicon/underfill, it was found both hygrothermal loading and thermal aging had significant effect. It was also found that thermal aging relieved the stresses induced by hygrothermal mismatch between dissimilar materials involved. As a result, thermal aging effectively prevented interfaces from the fracture propagation. Further study on fracture parameters presented the same trend as the conclusions made in strain gradients study. Since the magnitude of strains and SIFs of thermal aging and hygrothermal loading were quantitatively comparable, time effect was supposed to be considered in hygrothermal aging. The viscoelasticity nature of underfill was beneficial to assembly reliability since it reduced the strains and SIFs induced by material swelling during moisture immigration. In case of simulation of hygrothermal conditioning, the creep behavior of underfill material, i.e., viscoelastic properties of underfill material should be included to alleviate the potential fracture threat since time effect can do positive impact on reliability of the assembly.

The measured critical interfacial fracture toughness showed that moisture significantly reduced the interfacial strength with the comparison of our previous study. The interception of the inter- and intra-molecular hydrogen bonding provided by the hydroxyl groups was thought to take place with respect to wide range of mode mixity. By combining the interface toughness and the critical interfacial fracture toughness, it was concluded that the hygrothermal loading would increase the possibility of interfacial delamination in the flip chip package. From fracture morphology study, it was observed that granular bulges distributed over the whole interface of underfill part at 125 °C in our previous study. However, the surface without granula was seen for hygrothermal aged specimen tested under ambient condition. The observation indicated that moisture severed the chemical bonding, e.g., hydrogen bonding, between silicon/underfill and decreased the debonding stresses lower than yield stresses of underfill material locally.

## References


[1] X. J. Fan, H. B. Wang, and T. B. Lim, "Investigation of the underfill delamination and cracking for flip chip module during thermal cyclic loading," *IEEE Trans. Compon. Packag. Technol.*, vol. 24, no. 1, pp. 84–91, Mar. 2001.

[2] G. Q. Zhang, W. D. van Driel, and X. J. Fan, *Mechanics of Microelectronics*. New York: Springer, 2006.

[3] X. J. Fan, J. Zhou, G. Q. Zhang, and L. J. Ernst, "A micromechanics based vapor pressure model in electronic packages," *ASME J. Electron. Packag.*, vol. 127, pp. 262–267, 2005.

[4] T. Ferguson and J. M. Qu, "Effect of moisture on the interfacial adhesion of the underfill/solder mask interface," *J. Electron. Packag.*, vol. 124, pp. 106–110, 2002.

[5] J. H. Okura, A. Dasgupta, and J. F. J. M. Caers, "Hygro-mechanical durability of underfilled flip-chip-on-board (FCOB) interconnects," *J. Electron. Packag.*, vol. 124, pp. 184–187, 2002.

[6] X. J. Fan, G. Q. Zhang, and L. J. Ernst, "Interfacial delamination mechanisms during reflow with moisture preconditioning," *IEEE Trans. Compon. Packag. Technol.*, vol. 31, no. 1, Mar. 2008, to be published.

[7] B. Xie, X. Q. Shi, and X. J. Fan, "Sensitivity investigation of substrate thickness and reflow profile on wafer level film failures in 3D chip scale packages by finite element modeling," in *Proc. 57th Electron. Comp. Technol. Conf.*, Sparks, NV, May/Jun. 29–1, 2007, pp. 242–248.

[8] B. Xie, X. Q. Shi, and X. J. Fan, "Accelerated moisture sensitivity test methodology for stacked-die molded matrix array package," in *Proc. 9th Electron. Packag. Technol. Conf.*, Singapore, Dec. 10–12, 2007.

[9] C. E. Park, B. J. Han, and H. E. Bair, "Humidity effect on adhesion strength between solder ball and epoxy underfills," *Polymer*, vol. 38, no. 15, pp. 3811–3818, 1997.

[10] A. Kuhl and J. M. Qu, "A technique to measure interfacial toughness over a range of phase angles," *J. Electron. Packag.*, vol. 122, pp. 147–151, 2000.

[11] J. R. Rice, "Elastic fracture mechanics concepts for interfacial cracks," *J. Appl. Mech.*, vol. 55, pp. 98–10, 1988.

[12] J. Dunders, "Edge-bonded dissimilar orthogonal elastic wedges," *J. Appl. Mech.*, vol. 36, pp. 650–652, 1969.

[13] D. R. J. Owen and A. J. Fawkes, *Engineering Fracture Mechanics: Numerical Methods and Applications*. Swansea, U.K.: Pineridge Press, 1983.

[14] M. L. Williams, "The stresses around a fault of crack in dissimilar media," *Bull. Seismol. Soc. Amer.*, vol. 49, pp. 199–204, 1959.

[15] X. Q. Shi, Z. P. Wang, and J. P. Pickering, "A new methodology for the characterization of fracture toughness of filled epoxy films involved in microelectronics packages," *Microelectron. Reliab.*, vol. 43, pp. 1105–1115, 2003.

[16] D. Post, B. Han, and P. Ifju, *High Sensitivity Moiré: Experimental Analysis for Mechanics and Materials*. New York: Springer–Verglag, 1994.

[17] H. A. Bruck, S. R. McNeill, M. A. Sutton, and W. H. Peters, "Digital image correlation using newton-raphson method of partial differential correlation," *Exp. Mech.*, vol. 29, pp. 261–267, 1989.

[18] X. Q. Shi, Y. L. Zhang, and W. Zhou, "Determination of fracture toughness of polymer/inorganic interface with digital image speckle correlation technique," *IEEE Trans. Compon. Packag. Technol.*, vol. 30, no. 1, pp. 101–109, Mar. 2007.

[19] X. Q. Shi, H. L. J. Pang, X. R. Zhang, Q. J. Liu, and M. Ying, "*In-situ* micro-digital image speckle correlation technique for characterization of materials' properties and verification of numerical models," *IEEE Trans. Compon. Packag. Technol.*, vol. 27, no. 4, pp. 659–667, Dec. 2004.

[20] W. Zhang, D. Wu, B. Su, S. A. Hareb, Y. C. Lee, and B. P. Materson, "The effect of underfill epoxy on warpage in flip chip assemblies," *IEEE Trans. Compon., Packag., Manufact. Technol. A*, vol. 21, no. 2, pp. 323–328, Jun. 1998.

[21] X. Q. Shi, Z. P. Wang, H. L. J. Pang, and X. R. Zhang, "Investigation of effect of temperature and strain rate on mechanical properties of underfill material by use of microtensile specimens," *Polymer Testing*, vol. 21, pp. 725–733, 2002.

[22] X. Q. Shi, Y. L. Zhang, and W. Zhou, "Reliability study of underfill/chip interface with multifunctional micro-moiré interferometry system," *Microelectron. Reliab.*, vol. 46, no. 2-4, pp. 409–420, 2006.

[23] S. Y. Kook, J. M. Snodgrass, A. Kirtikar, and R. H. Dauskardt, "Adhesion and reliability of polymer/inorganic interfaces," *J. Electron. Packag.*, vol. 120, pp. 328–334, 1998.

[24] J. W. Hutchinson and Z. G. Suo, "Mixed mode cracking in layered materials," *Adv. Appl. Mech.*, vol. 29, pp. 63–191, 1992.

[25] T. K. Kwei, *J. Appl. Polym. Sci.*, vol. 10, pp. 1647–1647, 1966.

[26] G. Z. Xiao and W. E. R. Shanahan, "Swelling of DGEBA/DDA epoxy resin during hygrothermal aging," *Polymer*, vol. 39, no. 14, pp. 3253–3260, 1998.

[27] J. Crank, *The Mathematics of Diffusion*, 2nd ed. Oxford, U.K.: Oxford Univ. Press, 1975.

[28] J. Wang, Z. Qian, D. Zou, and S. Liu, "Creep behavior of a flip-chip package by both fem modeling and real time moiré interferometry," *J. Electron. Packag.*, vol. 120, pp. 179–185, 1998.

[29] Y. Sung, J. S. Goh, and J. C. Yang, "Residual stresses in plastic IC packages during surface mounting process preceded by moisture soaking testing," *IEEE Trans. Compon., Packag., Manufact. Technol. B*, vol. 20, no. 3, pp. 247–254, Aug. 1997.

[30] C. K. Gurumurthy, E. J. Kramer, and C. Y. Hui, "Water-assisted subcritical crack growth along an interface between polyimide passivation and epoxy underfill," *Int. J. Fract.*, vol. 109, pp. 1–28, 2001.

[31] Y. L. Zhang, X. Q. Shi, and W. Zhou, "Determination of fracture toughness of underfill/chip interface with digital image speckle correlation technique," in *Proc. Electron. Comp. Technol. Conf.*, 2004, vol. 1, pp. 140–147.

[32] A. J. Kinloch, *Adhesion and Adhesives: Science and Technology*. New York: Chapman and Hall, 1987.

**Xunqing Q. Shi** received the Ph.D. degree from Tsinghua University, Beijing, China, in 1995.

He is now a Senior Manager with the Applied Science and Technology Research Institute, Hong Kong, China and a Guest Professor with the Shanghai Jiaotong University, Shanghai, China, and the Beijing University of Technology. His recent research interests are in the areas of 3-D packaging, micro- and nano-mechanics, electronic materials damage, fracture and failure mechanisms, and reliability of advanced electronic packaging.

**Yanlie L. Zhang** received the B.S. degree in civil engineering from Shanghai Jiao Tong University, Shanghai, China, in 2001 and the Ph.D. degree in mechanical engineering from Nanyang Technological University, Singapore, in 2006.

Since then he has been employed in the semiconductor manufacturing industry as a Research Engineer. His research interests include reliability of microelectronic packaging under thermal or hygrothermal testing environment and development of test methodologies applied in these tests.

Dr. Zhang received the Outstanding Student Paper Award of the IEEE Electronic Packaging Technology Conference in 2004.

**Wei Zhou** received the Ph.D. degree from Cambridge University, Cambridge, U.K., in 1991.

He worked in the Fraunhofer Institute for Mechanics of Materials, Freiburg, Germany, for one year and then went to work in Singapore. In 2002, he took sabbatical leave at Harvard University, Cambridge, MA, as a Visiting Scholar in Applied Physics. He is an Associate Professor with Nanyang Technological University, Singapore and also holds the position of Director of the Precision Engineering and Nanotechnology Center. His research interest lies mainly in FIB nanofabrication and materials processing.

**Xuejun J. Fan** received the B.S. and M.S. degrees from Tianjin University, Tianjin, China, in 1986 and 1984, respectively, and the Ph.D. degree in engineering mechanics from Tsinghua University, Beijing, China, in 1989.

He is currently an Associate Professor with the Department of Mechanical Engineering, Lamar University, Beaumont, TX. From 1997 to 2000, he was with the Institute of Microelectronics (IME), Singapore, heading the Modeling and Simulation in Advanced Packaging Development Group. He moved to Philips Research Lab, Briarcliff Manor, NY, as a Senior Member Research Staff in 2000, and then to Intel Cooperation, Chandler, AZ, as a Senior Staff Engineer in 2004. He has published more than 80 scientific papers and filed 14 U.S. patents.